Bidirectional Molecular Motors by Controlling Threading and Dethreading Pathways of a Linked Rotaxane

Hiromichi V. Miyagishi[1,2], Hiroshi Masai[1,3], and Jun Terao[1,*]

[1] Department of Basic Science, Graduate School of Arts and Sciences, The University of Tokyo.

[2] Current affiliation: Department of Chemistry, Faculty of Science, Hokkaido University.

[3] PRESTO, Japan Science and Technology Agency.

*cterao@mail.ecc.u-tokyo.ac.jp

Summary

Artificial molecular motors have attracted significant attention as models of biological machines and molecular motors. Unlike conventional artificial molecular motors, which rely on covalent bond rotation, molecular motors with mechanically interlocked molecules (MIM) generate significant rotational motion via the dynamic shuttling of the macrocyclic components and have thus attracted considerable attention. The topology of MIM-type molecular motors is currently limited to catenane structures, which require intricate synthetic procedures that typically produce a low synthetic yield. In this study, we develop a novel class of MIM-type molecular motors based on a rotaxane-type topology. The switching of the rotaxane threading/dethreading pathway of the linked rotaxane by protection/deprotection of the bulky stopper group and changes in solvent polarity enabled unidirectional rotation of the molecular motor. Detailed spectroscopic investigations provide a quantitative evaluation of the threading/dethreading reaction rates. Repeated unidirectional rotation and switching of the direction of rotation is achieved by controlling the reaction rates. Our findings demonstrate that linked rotaxanes can serve as MIM-type molecular motors whose rotation direction can be switched by controlling the threading/dethreading reactions; these motors are expected to find applications as a component of molecular machinery.

Introduction

Molecular motors, nanomachines that convert chemical to rotational energy, are ubiquitous in biological systems.[1,2] Artificial molecular motors provide insights into the dynamics of biological systems at the molecular level, and have attracted significant attention owing to their expected applications in dynamic functional materials.[3–7] Molecular motor systems can be constructed using several scaffolds. The earliest artificial molecular motors relied on light-driven unidirectional rotation around a double bond[8–12] or chemical fuel-induced unidirectional rotation around a single bond[13–17] (Figure 1A). Several dynamic materials incorporating these motors have been developed including actuators.[18–20] Conversely, a newer class of artificial molecular motors consisting of mechanically interlocked molecules (MIMs) undergo large rotational motion driven by the dynamic shuttling of macrocyclic components.[21–26] Notably, MIM-type molecular motors are the sole structural motif in which the direction of rotational motion can be switched,[22] demonstrating their potential applications in advanced functional molecular machinery. The unidirectional

rotational motion of MIM-type molecular motors is driven by the ratchet mechanism.[3,27] The fundamental unidirectional motion of macrocycles has been thoroughly exploited in molecular pumps, while several examples of unidirectional motion along the axles of rotaxanes and pseudorotaxanes are known.[7,24,28–38] However, the rotational cycle of motion in rotaxanes can only be completed by dethreading of the macrocycle from the axle owing to the finite axle length(Figure 1B); thus, rotaxanes are unsuitable for generating rotational motion. This problem can be overcome by connecting the ends of the axle to form a catenane structure to solve this problem (Figure 1C).[3] The cyclic topology of the "rail" component enables the macrocycle to undergo infinite unidirectional and rotational motion; however, this limits the topology of such MIM-type molecular motors to catenane-based motifs, which, in turn, limits the application scope of these motors because catenane-type molecular motors typically have complex structures and require intricate synthesis procedures owing to the size of the interlocked structures. The development of MIM-type molecular motors with simple structures is therefore in high demand.

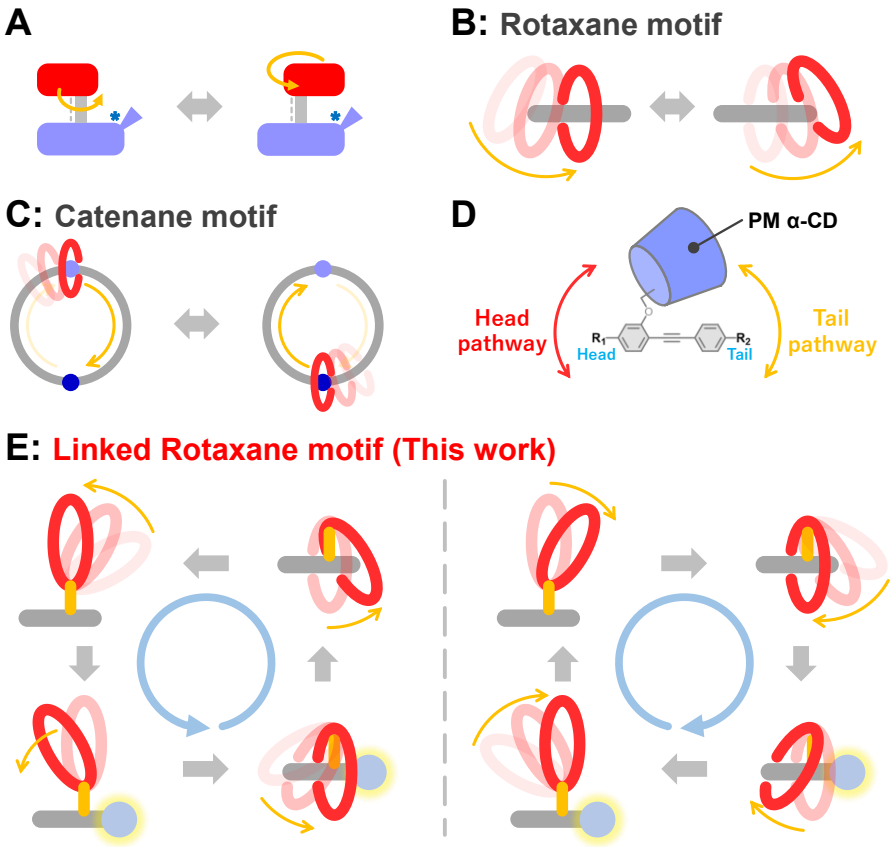

Figure 1. Schematic illustration of (A) single/double bond-type molecular motor, (B) unidirectional linear motion of pseudorotaxane macrocycles, and (C) catenane-type molecular motor. (D) Two threading/dethreading pathways of linked rotaxane with PM α-CD and DPA. (E) Schematic illustration of linked rotaxane-type molecular motor

Our group has developed numerous linked rotaxanes using permethylated α-cyclodextrin (PM α-CD) and diphenylacetylene (DPA).[39–47] The linked rotaxane can be switched between the inclusion and uninclusion structures by adjusting the solvent polarity. [40,48–51] The threading/dethreading processes occur via two pathways: the head and tail pathways. The threading/dethreading rates of both pathways are influenced by the size of the substituent on DPA (Figure 1D).[49,51] We therefore envisaged that alternating

between threading via the head pathway and dethreading via the tail pathway in PM α-CD would generate rotational motion. Thus, we propose a novel MIM-type molecular motor paradigm based on the linked rotaxane structure (Figure 1E). The dethreading event does not decompose the linked rotaxane structure into its constituent ring and axle components; hence, unidirectional rotation can be achieved by a succession of selective threading/dethreading reactions. Protection and deprotection of the linked rotaxane structure with bulky Fmoc groups is achieved by changing solvent polarity, which instigates threading through the head pathway and dethreading through the tail pathway, respectively, thereby achieving rotational motion.

Results and Discussion

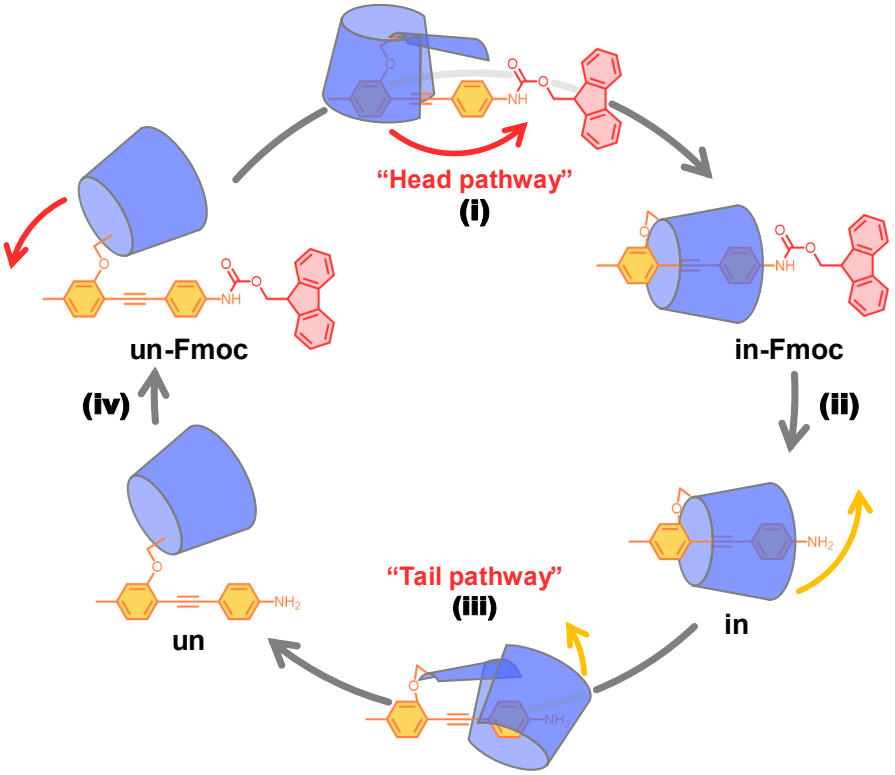

Figure 2. Mechanism of unidirectional rotation in the linked rotaxane-type molecular motor

The structure and rotation mechanisms of linked rotaxane-type molecular motors are shown in Figure 2. The introduction of a bulky Fmoc group at one end of DPA inhibits threading/dethreading via the tail pathway; thus, the reaction proceeds via the head pathway at the other side of DPA, which has a small, inert methyl group. In contrast, removal of the Fmoc protecting group to generate the amino group increases the rate of threading/dethreading via the tail pathway such that this mechanism is favored over the head pathway, resulting in threading/dethreading reactions via the tail pathway. The pathways of threading/dethreading pathway depends on the steric bulk of the tail end of the DPA; hence, the unidirectional rotation of the PM α-CD ring around the DPA axle can be achieved by insertion and removal of the Fmoc protecting groups to control the threading/dethreading pathways and alternating the solvent polarity to control the equilibrium between the inclusion and uninclusion structures (Figure 2)[49,51] Unidirectional rotation proceeds via a mechanism involving the following four steps, (i) the self-inclusion

reaction of **un-Fmoc** via the head pathway, yielding **in-Fmoc**; (ii) deprotection of **in-Fmoc** to yield **in**; (iii) dethreading of **in** via the tail pathway to yield **un**, and; (iv) protection of **un** with Fmoc to yield **un-Fmoc**. The synthesis of **un** is depicted in Scheme S1. Williamson ether synthesis using **1** and 6-*O*-monotosyl PM α-CD, followed by Sonogashira coupling, yielded **3**. The subsequent reduction of the nitro group and addition of the Fmoc protection group yielded **un-Fmoc** in four steps in 68% overall yield. To the best of our knowledge, this is the simplest and highest yielding synthesis of an MIM-type molecular motor (Table S2).[21–26]

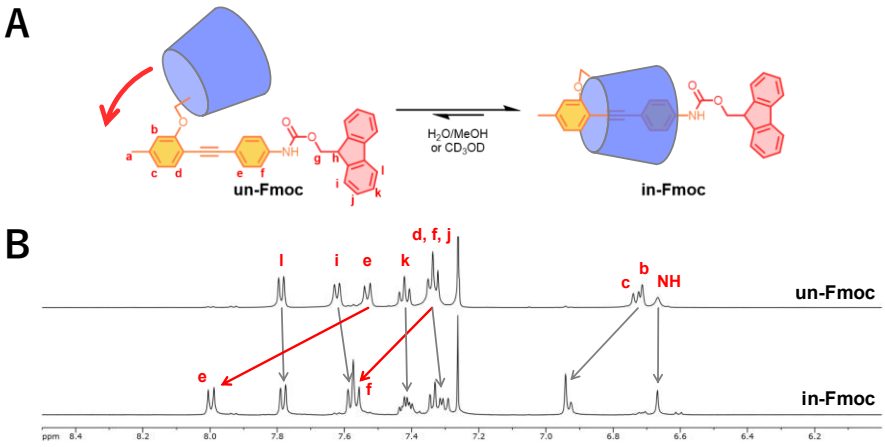

k_{in} / 10^4 s^{-1}	k_{out} / 10^4 s^{-1}
2.8	1.1

333 K, in CD_3OD

Figure 3. (A) Threading/dethreading reactions of **un**/**in-Fmoc**. (B) ^{1}H NMR spectra (500 MHz, $CDCl_3$) before and after the self-inclusion reaction in H_2O/MeOH (2:1) at 373 K. (C) Rate constants of the self-inclusion reaction of **un**/**in-Fmoc** in CD_3OD at 333 K

The first step of unidirectional rotation was achieved using the self-inclusion reaction via the head pathway by heating **un-Fmoc** in a mixed solvent of H_2O and methanol (Figure 3). The proton signals from the inner cavity of PM α-CD shifted downfield during the self-inclusion reaction, suggesting the formation of a linked rotaxane structure (Figure 3B).[45] In addition, the mechanostereochemistry of **un-Fmoc** and **in-Fmoc** was determined from their ROESY spectra (Figure S1). The ROESY spectrum of **in-Fmoc** showed the presence of strong nuclear Overhauser effects (NOE) between the protons of DPA and the H_5 protons located in the cavity of PM α-CD. In contrast, the ROESY spectrum of **un-Fmoc** showed a NOE between the protons of DPA and the H_4 protons located outside the cavity of PM α-CD. These results suggest that **in-Fmoc** forms a linked rotaxane structure. To investigate the mechanism of the self-inclusion reaction, the ^{1}H NMR spectra of **un**/**in-Fmoc** in CD_3OD was monitored at 333 K (Figure S2). The kinetic parameters were evaluated using nonlinear least-squares fitting, assuming a first-order reaction. The threading rate k_{in} (2.8×10^{-4} s^{-1} at 333 K) is similar to the expected rate of threading/dethreading via the head pathway.[49] These results therefore indicate that the self-inclusion reactions of **un**/**in-Fmoc** proceed through the head pathway.

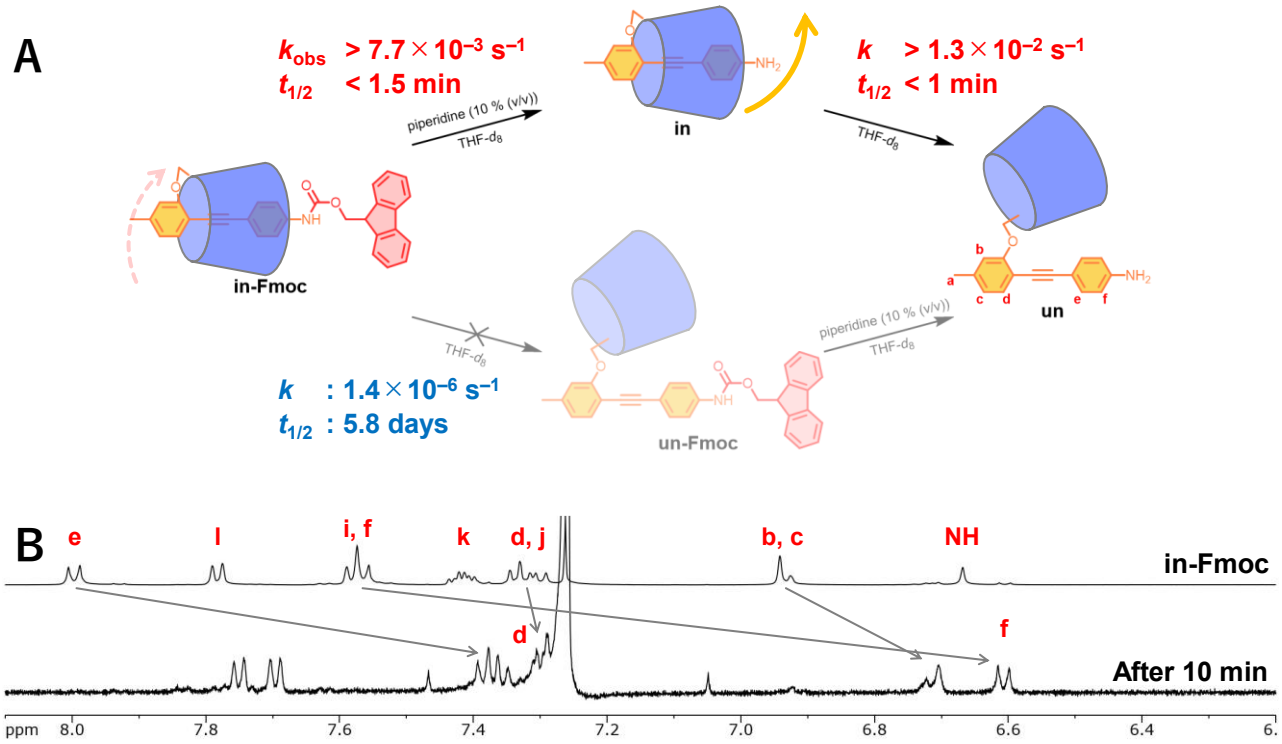

Figure 4. (A) Scheme of deprotection and subsequent dethreading of **in-Fmoc**. **in-Fmoc** can be converted to **un** via two possible routes. (B) ^{1}H NMR spectra before and after the deprotection and dethreading reactions in a solution of 10% (v/v) piperidine in THF (500 MHz, 303 K, $CDCl_3$)

To facilitate dethreading via the tail pathway, the Fmoc protecting group was removed from **in-Fmoc** in a solution of piperidine in THF (Figure 4A). **In-Fmoc** was completely converted to **un** within 10 min using a solution of 10% (v/v) piperidine in THF (Figure 4B). The estimated k_{obs} in this solution was estimated to be greater than 7.7 × 10^{-3} s^{-1}, assuming that the reaction proceeded to 99% completion within 10 min, whereas $t_{1/2}$ was less than 1.5 min. To confirm that the conversion of **in-Fmoc** to **un** proceeds through the tail pathway, the reaction rates of each individual step were evaluated (Figures 4, S3, and S4). The dethreading of **in** in THF-d_8 proceeded rapidly, as indicated by the high rate constant (k_{out} > 1.3 × 10^{-2} s^{-1}, $t_{1/2}$ < 1 min). Rapid dethreading of similar linked rotaxanes has been shown to proceed via the tail pathway.[51] In contrast, the dethreading of **in-Fmoc** was very slow (k_{out} = 1.4 × 10^{-6} s^{-1} and $t_{1/2}$ = 5.8 d, Figure S4), indicating that dethreading via the head pathway is associated with a high activation barrier. The conversion from **in-Fmoc** to **un** via the tail pathway was more than 1000 times faster than that through the head pathway (7.7 × 10^{-3} s^{-1} vs. 1.4 × 10^{-6} s^{-1}, Figure 4A), illustrating that dethreading via the head pathway dominates under these conditions. This kinetic asymmetry defines the direction of the rotational motion.

In the final step, the initial state of the molecular motor was established by introducing the bulky Fmoc protecting group into the tail end of **un** to yield **un-Fmoc** (Figure S5). ^{1}H NMR spectroscopy confirmed the formation of **un-Fmoc** and revealed that **un** was fully protected within 60 min. These results demonstrate that the PM α-CD moiety of the linked rotaxane underwent unidirectional rotation around DPA driven by successive Fmoc protection/deprotection and threading/dethreading reactions.

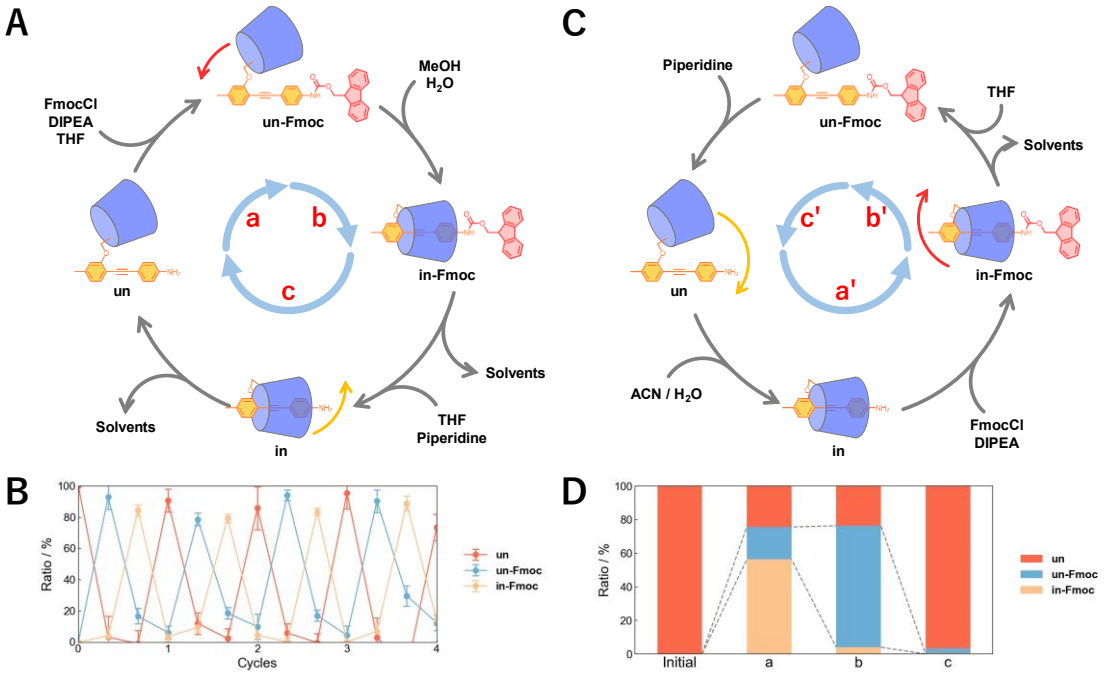

Figure 5. (A) Unidirectional rotation of the PM α-CD of **un** in a one-pot system and (B) abundance ratio of **un**, **un-Fmoc** and **in-Fmoc** in each step of the unidirectional rotation process. The error bars represent s. (C) Unidirectional rotation of the PM α-CD of **un** in the reverse direction and (D) abundance ratio of **un**, **un-Fmoc** and **in-Fmoc** in each step. a: FmocCl, DIPEA in THF, 60 °C,1 h; b: THF/MeOH/H_2O (1:6:9), 100 °C, 15 min, followed by solvent evaporation; c: piperidine in THF, 25 °C 1 h, followed by solvent evaporation, extraction by toluene/sat. NH_4Cl aq., and further solvent evaporation; a': FmocCl, DIPEA in ACN/H_2O (1:1), 60 °C, 1 h, followed by solvent evaporation, b': THF, 100 °C, 15 min, c': piperidine in THF, 25 °C, 30 min

Additionally, unidirectional rotation of the linked-rotaxane-type motors was achieved in a one-pot system (Figure 5A, B). First, **un** was protected with Fmoc in THF to yield **un-Fmoc** (step a), followed by the addition of MeOH/H_2O and heating at 100 °C to afford **in-Fmoc** (step b). The solvents were then removed before a solution of 10% (v/v) piperidine in THF was added to remove the Fmoc protecting group, allowing the dethreading reaction of **in** to proceed, yielding **un**, the initial state of the molecular motor (step c). Several washing procedures were required in the final step to remove trace amounts of piperidine, which removed Fmoc, resulting in the undesirable deprotection of the rotaxane. The one-pot reactions were monitored by ^{1}H NMR spectroscopy, which clearly indicated the alternate formation of **un**, **un-Fmoc**, and **in-Fmoc** in each step. Four full rotations of the α-CD moiety can be performed sustainably (Figure 5B). These results demonstrate that linked-rotaxane-type molecular motors unambiguously undergo unidirectional rotation in a one-pot system.

Finally, we demonstrated unidirectional rotation in the reverse direction (Figure 5C, D). The rotation of linked-rotaxane-type motors occurs via the threading of **un** in ACN/H_2O followed by the protection of **in** with Fmoc (step a'), dethreading of **in-Fmoc** (step b'), and deprotection of **un-Fmoc** (step c'). While a non-negligible amount of **un** and **un-Fmoc** did not undergo unidirectional rotation, the linked-rotaxane-type motors primarily underwent unidirectional rotation in the reverse direction (Figure 5D). The presence of residual **un** and **un-Fmoc** was attributed to the low polarity of the ACN/H_2O (1:1) solvent system;

however, this solvent system is considered optimal because further increasing the solvent polarity induces phase separation that reduces the yield of **in-Fmoc**. This switching of the unidirectional rotation direction of MIM-type molecular motors, which is a rare phenomenon,[22] demonstrates the advantage of molecular motors driven by sequential chemical reactions.

Conclusion

A rotaxane-type molecular motor was developed using PM α-CD and DPA. Protection/deprotection of the rotaxane structure with Fmoc enabled selective threading/dethreading reactions, resulting in unidirectional rotation of the PM α-CD moiety around DPA. The reaction rates in each step are indicative of the unidirectional motion of the motor. In addition, unidirectional rotation of the motor was achieved in both directions in a one-pot process. The structure of the linked-rotaxane-type molecular motor is less complex than that of conventional catenane-type molecular motors, which facilitates the application of MIM-type molecular motors in dynamic functional materials.

Experimental Procedures

Unidirectional rotation in a one-pot manner

To a solution of **un** (14.3 mg, 10.1 μmol) in THF (1 mL), DIPEA (3.74 μL, 22.0 μmol, 2.2 eq.) and FmocCl (5.2 mg, 20.1 μmol, 2.0 eq.) in a pressure vessel were added and stirred for 1 h at 60 °C. After the mixture cooled to room temperature, a 50 μL aliquot was taken, and NMR measurements ($CDCl_3$) were conducted after removing the solvent (**un-Fmoc**). Next, MeOH (5.7 mL) and H_2O (8.55 mL) were added to the mixture and stirred for 15 min at 100 °C. After cooling, a 50 μL aliquot was taken, and NMR measurements ($CDCl_3$) were conducted with similar procedures (**in-Fmoc**). Subsequently, the solvent was removed, followed by the addition of THF (810 μL) and piperidine (90 μL). The mixture was stirred for 1 h at 25 °C, a 50 μL aliquot was taken, and NMR measurements ($CDCl_3$) were conducted with similar procedures (**un**). The solvent was removed in vacuum, toluene (1 mL) and sat. NH_4Cl aq. (1 mL) were added, and the mixture was extracted with toluene (2 × 1 mL) in the pressure vessel to remove residual piperidine. Removal of solvent affords crude mixture of **un**, which was reintroduced into the initial step. The amounts of reagents were adjusted based on the amount of molecular motor, which decreases due to the sampling for NMR measurements (Table S1).

Unidirectional rotation in the reverse direction

To a solution of **un** (8.7 mg, 6.1 μmol) in ACN (4 mL) and H_2O (4 mL), DIPEA (3.37 μL, 19.8 μmol, 3.2 eq.) and FmocCl (4.6 mg, 17.8 μmol, 2.9 eq.) were added, and the mixture was stirred for 1 h at 60 °C. After the mixture cooled to room temperature, the solvent was evaporated and THF (6 mL) was added. A 50 μL aliquot was taken, and NMR measurements ($CDCl_3$) were conducted after removing the solvent (**in-Fmoc**). The mixture containing **in-Fmoc** was stirred for 15 min at 100 °C. After cooling, a 50 μL aliquot was taken, and NMR measurements ($CDCl_3$) were conducted with similar procedures (**un-Fmoc**). To the mixture, piperidine (222 μL) was added and the mixture was stirred for 30 min at 25 °C. Again, a 50 μL aliquot was

taken, and NMR measurements ($CDCl_3$) were conducted with similar procedures (**un**).

Acknowledgments

The authors acknowledge Dr. Susumu Tsuda for supplying PM α-CD derivatives. The authors would like to thank to Dr. Fumitaka Ishiwari for fruitful discussion. This research was supported by following financial supports (JSPS Research Fellow; JSPS KAKENHI Grant Numbers 21J14199, 21K05181, 21K18948, and 22H02060; JST CREST Grant Number JPMJCR19I2; NEDO Grant Number JPNP21016; Toshiaki Ogasawara Memorial Foundation; “Innovation inspired by Nature” Research Support Program, SEKISUI CHEMICAL CO., LTD.)

Author Contributions

H.V.M. and H.M. conceived the project. H.M. and J.T. supervised the project. H.V.M. performed the experiments, analyzed the data. All the authors have discussed the results and wrote the manuscript.

References

1. Schliwa, M., and Woehlke, G. (2003). Molecular motors. Nature *422*, 759–765.

2. Minamino, T., Imada, K., and Namba, K. (2008). Molecular motors of the bacterial flagella. Curr. Opin. Struct. Biol. *18*, 693–701.

3. Kassem, S., van Leeuwen, T., Lubbe, A.S., Wilson, M.R., Feringa, B.L., and Leigh, D.A. (2017). Artificial molecular motors. Chem. Soc. Rev. *46*, 2592–2621.

4. Roke, D., Wezenberg, S.J., and Feringa, B.L. (2018). Molecular rotary motors: Unidirectional motion around double bonds. Proc. Natl. Acad. Sci. U. S. A. *115*, 9423–9431.

5. Baroncini, M., Silvi, S., and Credi, A. (2020). Photo- and Redox-Driven Artificial Molecular Motors. Chem. Rev. *120*, 200–268.

6. García-López, V., Liu, D., and Tour, J.M. (2020). Light-Activated Organic Molecular Motors and Their Applications. Chem. Rev. *120*, 79–124.

7. Feng, Y., Ovalle, M., Seale, J.S.W., Lee, C.K., Kim, D.J., Astumian, R.D., and Stoddart, J.F. (2021). Molecular Pumps and Motors. J. Am. Chem. Soc. *143*, 5569–5591.

8. Koumura, N., Zijlstra, R.W., van Delden, R.A., Harada, N., and Feringa, B.L. (1999). Light-driven monodirectional molecular rotor. Nature *401*, 152–155.

9. Koumura, N., Geertsema, E.M., van Gelder, M.B., Meetsma, A., and Feringa, B.L. (2002). Second generation light-driven molecular motors. Unidirectional rotation controlled by a single stereogenic center with near-perfect photoequilibria and acceleration of the speed of rotation by structural modification. J. Am. Chem. Soc. *124*, 5037–5051.

10. Greb, L., and Lehn, J.-M. (2014). Light-driven molecular motors: imines as four-step or two-step unidirectional rotors. J. Am. Chem. Soc. *136*, 13114–13117.

11. Guentner, M., Schildhauer, M., Thumser, S., Mayer, P., Stephenson, D., Mayer, P.J., and Dube, H. (2015). Sunlight-powered kHz rotation of a hemithioindigo-based molecular motor. Nat. Commun. *6*, 8406.

12. Bach, N.N., Josef, V., Maid, H., and Dube, H. (2022). Active Mechanical Threading by a Molecular Motor. Angew. Chem. Int. Ed Engl. *61*, e202201882.

13. Dahl, B.J., and Branchaud, B.P. (2004). Synthesis and characterization of a functionalized chiral biaryl capable of exhibiting unidirectional bond rotation. Tetrahedron Lett. *45*, 9599–9602.

14. Fletcher, S.P., Dumur, F., Pollard, M.M., and Feringa, B.L. (2005). A reversible, unidirectional molecular rotary motor driven by chemical energy. Science *310*, 80–82.

15. Zhang, Y., Chang, Z., Zhao, H., Crespi, S., Feringa, B.L., and Zhao, D. (2020). A chemically driven rotary molecular motor based on reversible lactone formation with perfect unidirectionality. Chem *6*, 2420–2429.

16. Borsley, S., Kreidt, E., Leigh, D.A., and Roberts, B.M.W. (2022). Autonomous fuelled directional rotation about a covalent single bond. Nature *604*, 80–85.

17. Mo, K., Zhang, Y., Dong, Z., Yang, Y., Ma, X., Feringa, B.L., and Zhao, D. (2022). Intrinsically unidirectional chemically fuelled rotary molecular motors. Nature *609*, 293–298.

18. Li, Q., Fuks, G., Moulin, E., Maaloum, M., Rawiso, M., Kulic, I., Foy, J.T., and Giuseppone, N. (2015). Macroscopic contraction of a gel induced by the integrated motion of light-driven molecular motors. Nat. Nanotechnol. *10*, 161–165.

19. Chen, J., Leung, F.K.-C., Stuart, M.C.A., Kajitani, T., Fukushima, T., van der Giessen, E., and Feringa, B.L. (2018). Artificial muscle-like function from hierarchical supramolecular assembly of photoresponsive molecular motors. Nat. Chem. *10*, 132–138.

20. Hou, J., Long, G., Zhao, W., Zhou, G., Liu, D., Broer, D.J., Feringa, B.L., and Chen, J. (2022). Phototriggered Complex Motion by Programmable Construction of Light-Driven Molecular Motors in Liquid Crystal Networks. J. Am. Chem. Soc. *144*, 6851–6860.

21. Leigh, D.A., Wong, J.K.Y., Dehez, F., and Zerbetto, F. (2003). Unidirectional rotation in a mechanically interlocked molecular rotor. Nature *424*, 174–179.

22. Hernández, J.V., Kay, E.R., and Leigh, D.A. (2004). A reversible synthetic rotary molecular motor. Science *306*, 1532–1537.

23. Wilson, M.R., Solà, J., Carlone, A., Goldup, S.M., Lebrasseur, N., and Leigh, D.A. (2016). An autonomous chemically fuelled small-molecule motor. Nature *534*, 235–240.

24. Erbas-Cakmak, S., Fielden, S.D.P., Karaca, U., Leigh, D.A., McTernan, C.T., Tetlow, D.J., and Wilson, M.R. (2017). Rotary and linear molecular motors driven by pulses of a chemical fuel. Science *358*, 340–343.

25. Zhang, L., Qiu, Y., Liu, W.-G., Chen, H., Shen, D., Song, B., Cai, K., Wu, H., Jiao, Y., Feng, Y., et al. (2023). An electric molecular motor. Nature *613*, 280–286.

26. Gallagher, J.M., Roberts, B.M.W., Borsley, S., and Leigh, D.A. (2023). Conformational selection accelerates catalysis by an organocatalytic molecular motor. Chem *0*. 10.1016/j.chempr.2023.10.019.

27. Sangchai, T., Al Shehimy, S., Penocchio, E., and Ragazzon, G. (2023). Artificial Molecular Ratchets: Tools Enabling Endergonic Processes. Angew. Chem. Int. Ed Engl., e202309501.

28. Qiu, Y., Feng, Y., Guo, Q.-H., Astumian, R.D., and Stoddart, J.F. (2020). Pumps through the Ages. Chem *6*, 1952–1977.

29. Arduini, A., Bussolati, R., Credi, A., Monaco, S., Secchi, A., Silvi, S., and Venturi, M. (2012). Solvent- and light-controlled unidirectional transit of a nonsymmetric molecular axle through a nonsymmetric molecular wheel. Chemistry *18*, 16203–16213.

30. Baroncini, M., Silvi, S., Venturi, M., and Credi, A. (2012). Photoactivated directionally controlled transit of a non-symmetric molecular axle through a macrocycle. Angew. Chem. Int. Ed Engl. *51*, 4223–4226.

31. Ragazzon, G., Baroncini, M., Silvi, S., Venturi, M., and Credi, A. (2015). Light-powered autonomous and directional molecular motion of a dissipative self-assembling system. Nat. Nanotechnol. *10*, 70–75.

32. Canton, M., Groppi, J., Casimiro, L., Corra, S., Baroncini, M., Silvi, S., and Credi, A. (2021). Second-Generation Light-Fueled Supramolecular Pump. J. Am. Chem. Soc. *143*, 10890–10894.

33. Li, H., Cheng, C., McGonigal, P.R., Fahrenbach, A.C., Frasconi, M., Liu, W.-G., Zhu, Z., Zhao, Y., Ke, C., Lei, J., et al. (2013). Relative unidirectional translation in an artificial molecular assembly fueled by light. J. Am. Chem. Soc. *135*, 18609–18620.

34. Cheng, C., McGonigal, P.R., Liu, W.-G., Li, H., Vermeulen, N.A., Ke, C., Frasconi, M., Stern, C.L., Goddard, W.A., 3rd, and Stoddart, J.F. (2014). Energetically demanding transport in a supramolecular assembly. J. Am. Chem. Soc. *136*, 14702–14705.

35. Cheng, C., McGonigal, P.R., Schneebeli, S.T., Li, H., Vermeulen, N.A., Ke, C., and Stoddart, J.F. (2015). An artificial molecular pump. Nat. Nanotechnol. *10*, 547–553.

36. Qiu, Y., Song, B., Pezzato, C., Shen, D., Liu, W., Zhang, L., Feng, Y., Guo, Q.-H., Cai, K., Li, W., et al. (2020). A precise polyrotaxane synthesizer. Science *368*, 1247–1253.

37. Amano, S., Fielden, S.D.P., and Leigh, D.A. (2021). A catalysis-driven artificial molecular pump. Nature *594*, 529–534.

38. David, A.H.G., García–Cerezo, P., Campaña, A.G., Santoyo–González, F., and Blanco, V. (2022). Vinyl sulfonyl chemistry-driven unidirectional transport of a macrocycle through a [2]rotaxane. Organic Chemistry Frontiers *9*, 633–642. 10.1039/d1qo01491a.

39. Terao, J., Tanaka, Y., Tsuda, S., Kambe, N., Taniguchi, M., Kawai, T., Saeki, A., and Seki, S. (2009). Insulated molecular wire with highly conductive pi-conjugated polymer core. J. Am. Chem. Soc. *131*, 18046–18047.

40. Terao, J. (2011). π-Conjugated molecules covered by permethylated cyclodextrins. Chem. Rec. *11*, 269–283.

41. Terao, J., Wadahama, A., Matono, A., Tada, T., Watanabe, S., Seki, S., Fujihara, T., and Tsuji, Y. (2013). Design principle for increasing charge mobility of π-conjugated polymers using regularly localized molecular orbitals. Nat. Commun. *4*, 1691.

42. Masai, H., Terao, J., Makuta, S., Tachibana, Y., Fujihara, T., and Tsuji, Y. (2014). Enhancement of phosphorescence and unimolecular behavior in the solid state by perfect insulation of platinum-acetylide polymers. J. Am. Chem. Soc. *136*, 14714–14717.

43. Masai, H., Yokoyama, T., Miyagishi, H.V., Liu, M., Tachibana, Y., Fujihara, T., Tsuji, Y., and Terao, J. (2020). Insulated conjugated bimetallopolymer with sigmoidal response by dual self-controlling system as a biomimetic material. Nat. Commun. *11*, 408.

44. Miyagishi, H.V., Masai, H., and Terao, J. (2020). Suppression of Undesirable Isomerization and Intermolecular Reactions of Double Bonds by a Linked Rotaxane Structure. Chem. Asian J. *15*, 1890–1895.

45. Miyagishi, H.V., Masai, H., and Terao, J. (2022). Linked Rotaxane Structure Restricts Local Molecular Motions in Solution to Enhance Fluorescence Properties of Tetraphenylethylene. Chem. Eur. J. *28*, e202103175.

46. Shimada, S., Miyagishi, H.V., Masai, H., Masui, Y., and Terao, J. (2022). Solvatofluorochromic contrast with supramolecular stereoisomers using linked rotaxane structures to investigate local solvation in excited donor-bridge-acceptor systems. Bull. Chem. Soc. Jpn. *95*, 163–168.

47. Chou, S.-Y., Masai, H., Otani, M., Miyagishi, H.V., Sakamoto, G., Yamada, Y., Kinoshita, Y., Tamiaki, H., Katase, T., Ohta, H., et al. (2023). Efficient electrocatalytic H2O2 evolution utilizing electron-

conducting molecular wires spatially separated by rotaxane encapsulation. Appl. Catal. B, 122373.

48. Tsuda, S., Terao, J., Tanaka, Y., Maekawa, T., and Kambe, N. (2009). Synthesis of linked symmetrical [3] and [5]rotaxanes having an oligomeric phenylene ethynylene (OPE) core skeleton as a π-conjugated guest via double intramolecular self-inclusion. Tetrahedron Lett. *50*, 1146–1150.

49. Masai, H., Terao, J., Fujihara, T., and Tsuji, Y. (2016). Rational Design for Rotaxane Synthesis through Intramolecular Slippage: Control of Activation Energy by Rigid Axle Length. Chem. Eur. J. *22*, 6624–6630.

50. Masai, H., and Terao, J. (2019). Synthetic Methodologies for Structurally Defined Linked-[n]Rotaxanes with Permethylated Cyclodextrins: Platform for Functionalized Molecular Electronics. Bull. Chem. Soc. Jpn. *92*, 529–539.

51. Ishino, S., Masai, H., Shimada, S., and Terao, J. (2020). Change in the rate of pseudo[1]rotaxane formation by elongating the alkyl-chain-substituted diphenylethynylene linked to permethyl α-cyclodextrin. Tetrahedron Lett. *61*, 152061.